Ab initio simulation of pressure-induced low-energy excitations in amorphous silicon

Murat Durandurdu and D. A. Drabold

Department of Physics and Astronomy, Condensed Matter and Surface Science Program, Ohio University, Athens, Ohio 45701-2979
(Received 22 April 2002; revised manuscript received 10 July 2002; published 10 October 2002)

We study the pressure dependence of vibrational spectrum of amorphous silicon using an *ab initio* constant pressure relaxation simulation. With the application of pressure the low-energy modes soften and their acousticlike character decreases. On the other hand, high-frequency modes shift toward the higher energies, and the localized spectral tail modes become extended under pressure.

I. INTRODUCTION

Extensive experimental and theoretical investigations have made considerable progress toward understanding the nature of vibrational dynamics of amorphous silicon (*a*-Si).[1–12] However, the changes in the vibrational spectrum of *a*-Si with external perturbations need to be explored. An investigation of *a*-Si under pressure is, therefore, important to understand not only changes in the vibrational spectrum but also the structure of *a*-Si.

a-Si can be prepared in various ways, which yields structures with different physical properties. It has been reported that the vibrational spectrum of *a*-Si depends on degree of structural disorder, sample preparation, deposition conditions, and hydrogen concentration.[1–3] The TA/TO intensity ratio and TO linewidth correlate with bond angle distribution of the sample.[3,6] The coordination defects lead to localized states not only near the high-frequency band edge, but also in the low-frequency tail.[7] There is a correlation between the density of *a*-Si and the number of localized states (the number of localized states decreases with increasing density of *a*-Si).[12] Nakhmanson and Drabold have shown that a fourfold coordinated model of *a*-Si does not exhibit low-energy excitations and that the presence of voids leads to extra low-energy states in the vibrational density of states[8] (VDOS) and a sharp peak in $C(T)/T$.[3,9]

Recently we showed that *a*-Si transformed via a first-order phase transition into an amorphous metallic phase using an *ab initio* constant pressure relaxation simulation,[13] which is in agreement with experiments.[14,15] Kelires[16] confirms an amorphous-to-amorphous phase transition in *a*-Ge and *a*-Si using an environment dependent interatomic potential (EDIP) and Tersoff potential. Kelires finds that the transition in both structures proceeds gradually and the free-energy calculation suggests a first-order transition in *a*-Si.[16] Since the behavior of *a*-Si under pressure is known from experimental and theoretical studies, *a*-Si is an excellent system to further study the phonon spectrum and states under pressure. In this paper, we present the pressure dependence of the low- and high-energy modes in *a*-Si using an *ab initio* constant pressure relaxation simulation and lattice-dynamical calculation. We find that pressure softens the low-energy modes and leads to a dramatic decrease in the acousticlike nature of these frequencies. The higher-frequency modes shift to larger energies up to the transition pressure at which point the mode frequencies decrease abruptly. The pressure-induced delocalization of highly localized high-frequency modes is observed with the application of pressure.

II. METHODOLOGY

The simulations reported here are carried out in a 216-atom model of *a*-Si. The *a*-Si model is by Djordjevic *et al.* and is in uniform agreement with structural, vibrational, and optical measurements.[17] At zero pressure, the *a*-Si model is relaxed with a local-orbital first-principles quantum dynamic method due to Sankey and Niklewski.[18] In this method, the local-density approximation to density-functional theory is used with a minimal basis of one *s* and three *p* pseudoatomic orbitals on each atom. These basis functions are slightly excited from their ground state and these are referred to as "fireball orbitals." The Harris functional with hard norm-conserving pseudopotentials is used. This method has been successfully applied in *c*-Si including high-pressure phases,[18] expanded volume phases of silicon ("zeolites without oxygen"),[19] and *a*-Si.[20,21] This Hamiltonian predicts successfully the pressure-induced phase transition in crystalline silicon (diamond to simple hexagonal) and in *a*-Si (amorphous to amorphous).[13] Slow dynamical quenching starting at 800 K under constant pressure is performed to fully relax the system to zero temperature. The number of steps required depends on pressure, and near the transition requires about 10 000 force calls. Pressure is applied via the method of Parrinello-Rahman[22] which enables the simulation cell to change volume and shape.

Once the equilibrium configurations under pressure are obtained, we compute the dynamical matrix, displacing every atom in the cell in three orthogonal directions (0.03 Å) and computing the resulting spring constants as second derivatives of the total energy of the system. Diagonalizing the dynamical matrix we receive its eigenvectors and corresponding squared normal-mode frequencies ω^2, which enables us to carry out a study of the vibrational behavior of the high-pressure configurations.

As a preliminary, we perform the calculation in a crystal silicon cell and find that the acoustic phonons are softened, while the optical phonons shift to higher energies,[13] which is consistent with Raman-scattering experiments.[23]

TABLE I. Structural properties of a-Si under pressure: average bond length (ABL), average bond angle (ABA), width of the bond angle distribution (WBAD), and average coordination number (ACN).

Pressure (GPa)	0	8	16	16.25	17
ABL (Å)	2.386	2.328	2.290	2.540	2.560
ABA	109.17°	108.93°	108.3 °	98.23°	97.88°
WBAD	11.1	12.1	14.2	32.9	33.0
ACN	4.0	4.0	4.1	8.6	9.2

III. RESULTS AND DISCUSSION

A. Vibrational density of states

First, we give a brief review of the structural properties of a-Si under pressure (Table I). The details of the pressure-induced phase transition of a-Si is reported in Ref. 13. The initial compression causes narrowed tetrahedral angles, shortened bond lengths, and a small increase in the coordination. At 16.25 GPa, a pressure-induced phase transition occurs with abrupt volume and topological change. At the transition, the average bond angle drops to 98.23° which is intermediate between the tetrahedral and octahedral values of 109.5° and 90°, respectively. The average bond length is 2.54 Å.

The vibrational density of states (VDOS) of a-Si under pressure is given in Fig. 1. At zero pressure a-Si shows no vibrational states present with energies below 60 cm^{-1} because of the finite size and ideal structure of the simulation cell:[9] small **k** acoustic modes are missing from our simulation which is strictly zone centered. As the applied pressure increases, the low-energy vibrational states shift to smaller
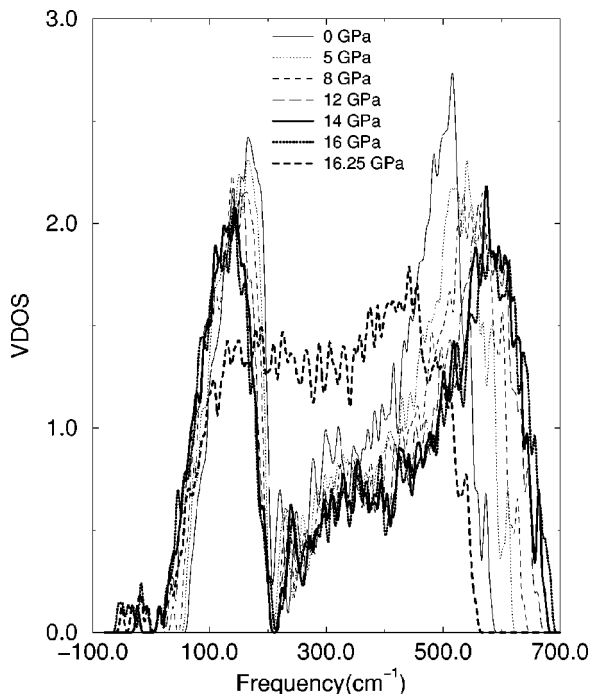

FIG. 1. The behavior of the VDOS under pressure.

energies. Near the transition pressure, there are negative squared eigenvalues ($\omega^2 < 0$) yielding imaginary frequencies. We have followed the method used in Ref. 24 and multiplied the imaginary frequencies by i so that they show up on the negative real frequency axis. At 14 GPa, an unstable frequency appears in the VDOS for the first time and the maximum unstable frequencies are observed at 16 GPa before the phase change. We also find that pressure pushes the frequency modes ($\omega > 200$ cm^{-1}) toward larger energies.

The behavior of modes in a-Si is very different from that of a-GeSe$_2$ (Ref. 25) and SiO$_2$,[26] in which the bands shift to higher frequencies without softening modes. The modification of the modes in a-Si can be understood by examining the Grüneisen parameter. Fabian and Allen[27] have shown that the low-frequency modes of a-Si have a negative Grüneisen parameter, which means that these modes soften with a decrease of volume.

B. Imaginary frequencies

In the study of coesite under pressure,[28] it was reported that the mechanical instability as indicated by imaginary frequencies and group velocities occurs near the coesite-stishovite phase boundary. Binggeli and Chelikowsky *et al.*[29] have shown that the instability is associated with vanishing acoustic velocities and leads to imaginary frequencies near Γ in the quartz phonon spectrum above the critical pressure. Lacks[30] reported that the decrease of a normal-mode frequency to zero implies that the dynamical matrix (Hessian) becomes nonpositive definite. This corresponds to disappearance of the local energy minimum. Afterwards the system becomes mechanically unstable and relaxes at an unrelated local minimum.

The existence of imaginary frequencies near the transition pressure is an artifact of the simulations because of the short-time scale of the simulations' exploration of configurational space. These imaginary frequencies, however, can be attributed to the mechanical instability of the model system. Although they are unphysical, for the model system they serve as a harbinger of mechanical instability. As reported in the study of silica under pressure,[30] the mechanical instabilities are irreversible, lead to discontinuous structural change, and are localized to small groups of atoms with different groups of atoms becoming unstable at different pressures. Also it is argued that pressure-induced amorphization and amorphous-to-amorphous transitions arise from the phonon softening and mechanical instability[31] which is consistent with the results obtained in the present study. However, further investigations are required to clarify these issues.

C. Phase quotient

In a crystal, vibrations can be explained with acoustic and optic phonons. In acoustic modes, neighboring atoms move in phase while in optic modes the motion is out of phase. In amorphous materials, the atomic vibrations cannot be characterized with a definite wave vector and a division of atomic vibration into acoustic and optic phonons is not possible in general.[32] However, some characteristics can be calculated for vibrational modes in amorphous materials. One
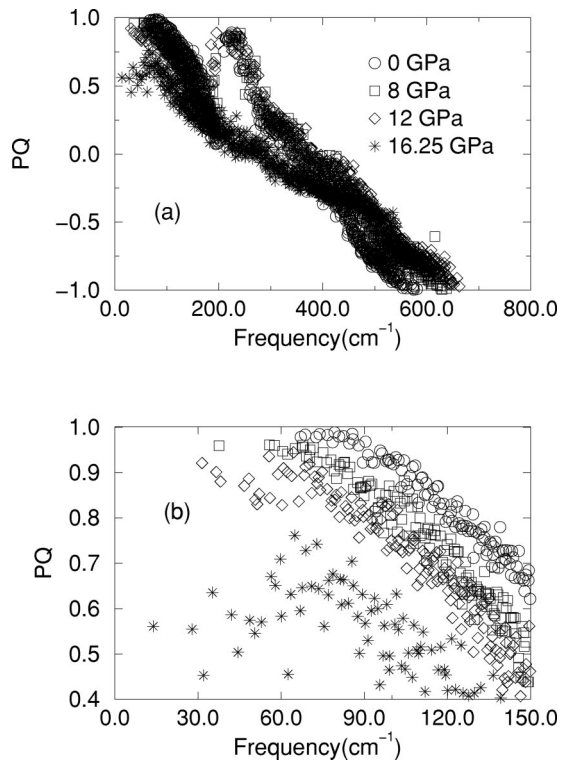
FIG. 2. The phase quotient, Eq. (1). The PQ is close to $+1$ for acousticlike modes and it is around -1 for opticlike modes.

FIG. 3. Stretching character of the vibrational modes, Eq. (2).

of the useful quantities is the phase quotient. The phase relationship between vibrations of neighboring atoms can be explained with the phase quotient (PQ):[11]

$$PQ(\omega_n) = \frac{\sum_m \mathbf{u}_n^i \cdot \mathbf{u}_n^j}{\sum_m |\mathbf{u}_n^i \cdot \mathbf{u}_n^j|}, \qquad (1)$$

where atoms i and j constitute the mth bond, $\mathbf{u}_n^i$ is the displacement of atom i from its equilibrium position when it vibrates in mode n, and the summation is over all nearest-neighbor bonds in the cluster. In terms of values of the phase quotient, it is possible to talk about acousticlike and opticlike modes in amorphous materials. In acousticlike modes, the motion of atoms i and the j is roughly in phase and the PQ is close to $+1$, and in opticlike phonons, the relative motion of atoms is roughly antiparallel for each pair and the PQ is around -1.

The pressure dependence of the PQ is depicted in Fig. 2. At zero pressure the vibrations with $\omega < 200$ cm^{-1} are acousticlike while the high-frequency spectral tail states have an opticlike character. The general features of the PQ at zero pressure are in agreement with a previous report.[11] With the application of pressure, the PQ exhibits a dramatic change at low energy: the PQ tends to decrease under pressure, indicating a decrease in the acousticlike nature of these eigenmodes. After the network undergoes a phase transition, the PQ at the low-energy part declines dramatically (PQ~0.5),
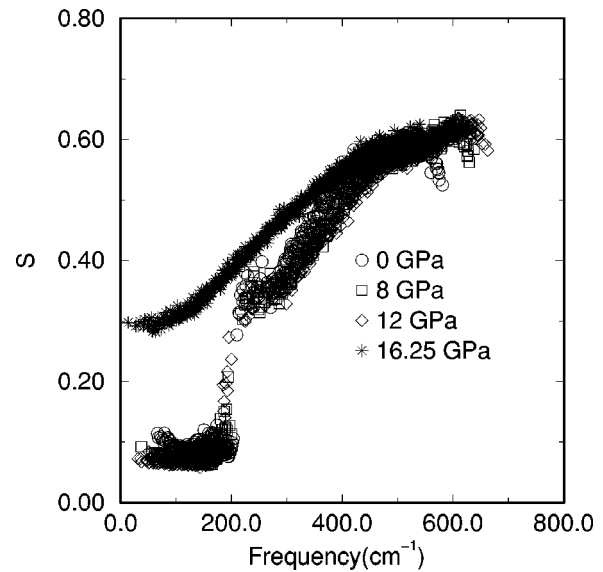
implying that a high coordination of the structure yields an increase of the opticlike nature of the low-energy modes.

D. Stretching character

The stretching character $S(\omega)$ can be given by

$$S(\omega_n) = \frac{\sum_m |(\mathbf{u}_n^i - \mathbf{u}_n^j) \cdot \mathbf{r}^m|}{\sum_m |\mathbf{u}_n^i - \mathbf{u}_n^j|}, \qquad (2)$$

where $\mathbf{r}^m$ is a unit vector parallel to the mth bond (see Ref. 11). $S(\omega)$ is close to unity if the mode n is predominantly of a bond-stretching character and close to 0 if the n mode is a bond-bending type.

The pressure dependence of $S(\omega)$ is given in Fig. 3. The modes less than 200 cm^{-1} have a bond-bending character while the phonons above 200 cm^{-1} have a bond-stretching character. As pressure increases a small change of $S(\omega)$ is seen up to the transition pressure. At transition $S(\omega)$ shows very dramatic modification ($\omega < 400$ cm^{-1}) and all modes have a bond-stretching character.

E. Localized states and response to pressure

The usual measure of the degree of localization of vibrational modes is the inverse participation ratio (IPR) P^{-1},

$$P^{-1}(\omega_n) = N \sum_{j=1}^{N} (\mathbf{u}_n^j \cdot \mathbf{u}_n^j)^2 \left[\sum_{j=1}^{N} (\mathbf{u}_n^j \cdot \mathbf{u}_n^j) \right]^{-2}, \qquad (3)$$

where N is the number of atoms in the supercell and $\mathbf{u}_n$ is the displacement of atom j from its equilibrium position. The IPR will have a value of ~ 1 for an extended mode where all atoms contribute equally and a value of $1/N$ for a mode
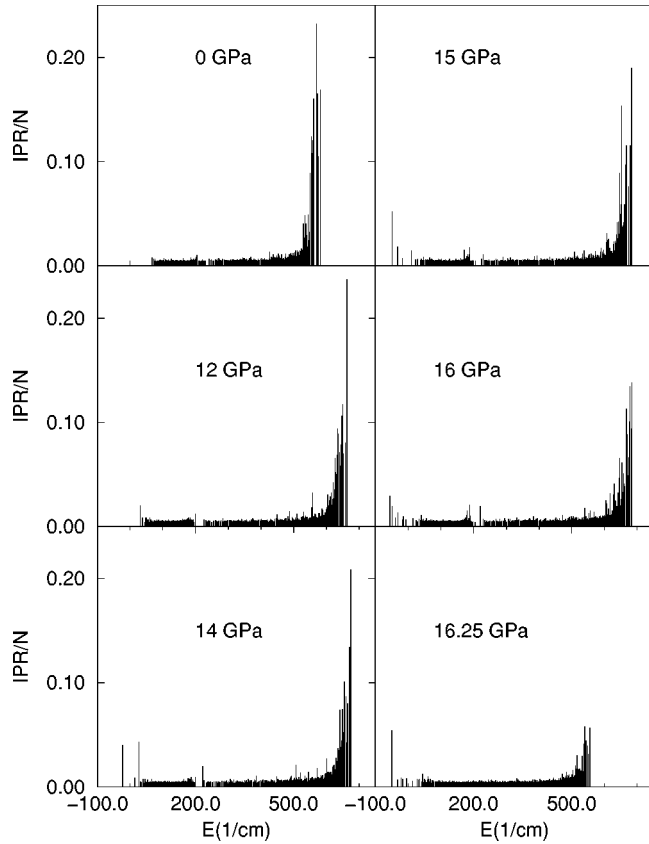
FIG. 4. The inverse participation ratio of the a-Si modes under pressure. Note that the low-energy states are completely extended and the high-energy modes are localized at zero pressure.

FIG. 5. The black, gray, and white atoms correspond to $\geq 10\%$, $\geq 5\%$, and $\leq 5\%$ of the total excitation, respectively. (a) $\omega = 37.63$ cm^{-1} at 8 GPa, (b) $\omega = 31.47$ cm^{-1} at 12 GPa, (c) $i\omega = -23.0$ cm^{-1} at 14 GPa, (d) $\omega = 26.57$ cm^{-1} at 14 GPa, (e) $i\omega = -49.26$ cm^{-1} at 15 GPa, and (f) $i\omega = -32.22$ cm^{-1} at 15 GPa. These modes with high IPR's at the low-energy regime are extended since the excitation is rather uniformly distributed.

defined by only one atom. In Fig. 4 we have the IPR of a-Si under pressure. In the figure each peak represents a single eigenmode. The larger the IPR for a state, the more it is spatially localized. At zero pressure all states except those at highest frequency are extended. The localized spectral tail states are extended with increasing pressure and they move into higher frequencies up to the transition pressure. At this pressure the states shift in the lower frequencies because of the abrupt structural change of the network. The delocalization of high-energy states under pressure has been reported in SiO$_2$ (Ref. 26) and a-GeSe$_2$.[25]

On the other hand, the low-frequency modes shift to smaller energies and a few of the states have a high IPR at 14 and 15 GPa. The eigenmodes at low frequencies, except for the first eigenmode, are delocalized at transition pressure. In order to understand whether these high IPR states at 14 GPa and 15 GPa are spatially localized or delocalized we visualize the states in two steps: (i) the eigenvector associated with each atom site is calculated for a given eigenvalue, and (ii) each atom is then drawn in one of the three levels of the gray scale according to the amount of eigenvector (squared component) associated with it. Very dark atoms represent strongly localized sites that contribute more than 10% of the total excitation, less dark atoms are the sites that contribute more than 5%, and the white atoms contribute the rest in Fig. 5. The gray scale map enables us to predict where the
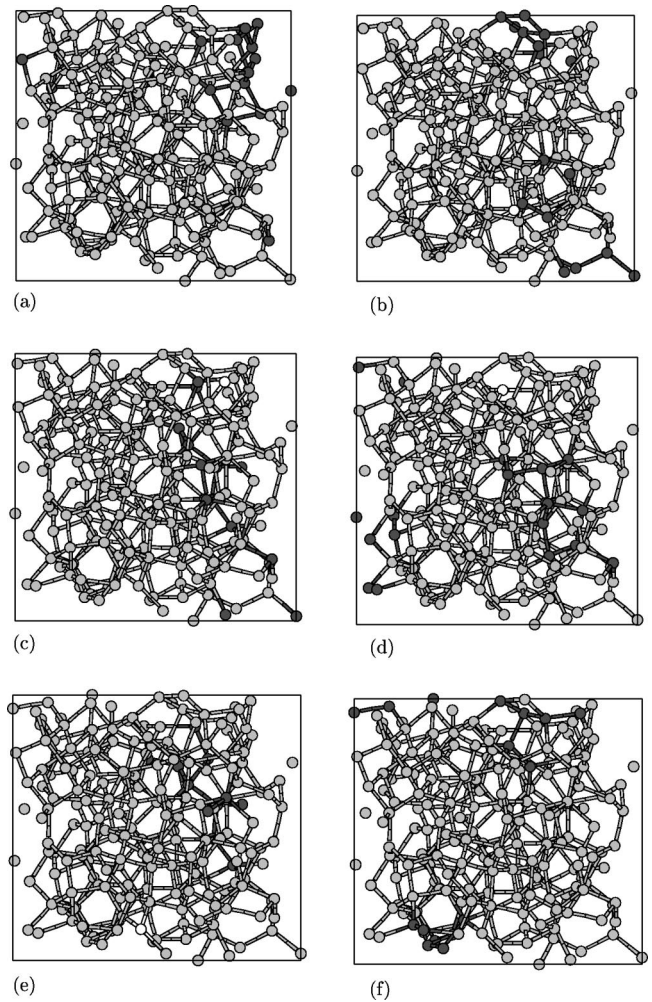
vibrations are localized and how they decay in space. In the figure, approximately 10–20 atoms (very dark) show strongly localized sites and they are associated with a large deviation of the bond angle from the ideal tetrahedral angle. Those atoms are involved with the mechanical instability. The excitations are rather uniformly distributed in space, indicating that these unstable modes are extended. In the study of liquid-glass transition,[33] it was reported that when the delocalized unstable modes show up at high temperatures, then a continuous flow mechanism for diffusion would be possible.

IV. CONCLUSIONS

Pressure dependence of the vibration spectrum of a-Si has been studied using an *ab initio* constant pressure relaxation

simulation. Pressure leads to extra low-energy states and reduces the acousticlike nature of these states. Up to the transition pressure, the high-frequency modes shift into larger values. It is found that the localized high-frequency states at zero pressure are extended with the application of pressure.

[1] S. Lannin, L.J. Pilione, S.T. Kshirsagar, R. Messier, and R.C. Ross, Phys. Rev. B **26**, 3506 (1982).

[2] N. Maley and J.S. Lannin, Phys. Rev. B **36**, 1146 (1987).

[3] N. Maley, D. Beeman, and J.S. Lannin, Phys. Rev. B **38**, 10 611 (1988).

[4] X. Liu, B.E. White, R.O. Pohl, E. Iwanizcko, K.M. Jones, A.H. Mahan, B.N. Nelson, R.S. Crandall, and S. Veprek, Phys. Rev. Lett. **78**, 4418 (1997).

[5] X. Liu and R.O. Pohl, Phys. Rev. B **58**, 9067 (1998).

[6] D. Beeman, R. Tsu, and M.F. Torpe, Phys. Rev. B **32**, 874 (1985).

[7] R. Biswas, A.A.M. Bouchard, W.A. Katmitakara, G.S. Grest, and C.M. Shoukolis, Phys. Rev. Lett. **60**, 2280 (1988).

[8] S. Nakhmanson and D.A. Drabold, Phys. Rev. B **58**, 15 325 (1998).

[9] S. Nakhmanson and D.A. Drabold, Phys. Rev. B **61**, 5376 (2000).

[10] J.L. Feldman, P.B. Allen, and S.R. Birkham, Phys. Rev. B **59**, 3551 (1999).

[11] M. Marinov and N. Zotov, Phys. Rev. B **55**, 2938 (1997).

[12] F. Finkemeier and W. von Niessen, Phys. Rev. B **58**, 4473 (1998).

[13] M. Durandurdu and D.A. Drabold, Phys. Rev. B **64**, 014101 (2001).

[14] O. Shimomura, S. Minomura, N. Sakai, K. Asaumi, K. Tamura, J. Fukushima, and H. Endo, Philos. Mag. **29**, 547 (1974).

[15] S. Minomura, *High Pressure and Low-Temperature Physics* (Plenum, New York, 1978), p. 483.

[16] P. C. Kelires, *CECAM Workshop on Rigidity and Strain Fields in Crystalline and Amorphous Materials*, *June 25–27, 2001, Lyon, France* (unpublished).

[17] B.R. Djordjevic, M.F. Thorpe, and F. Wooten, Phys. Rev. B **52**, 5685 (1995).

[18] O.F. Sankey and D.J. Niklewski, Phys. Rev. B **40**, 3979 (1989).

[19] A.A. Demkov, W. Windl, and O.F. Sankey Phys. Rev. B **53**, 11 288 (1996).

[20] P.A. Fedders, D.A. Drabold, and S. Nakhmanson, Phys. Rev. B **58**, 15 624 (1998).

[21] M. Durandurdu, D.A. Drabold, and N. Mousseau, Phys. Rev. B **62**, 15 307 (2000).

[22] M. Parrinello and A. Rahman, Phys. Rev. Lett. **45**, 1196 (1980).

[23] B. Weinstein and G.J. Piermarini, Phys. Rev. B **12**, 1172 (1975).

[24] S.D. Bembenek and B.B. Laird, Phys. Rev. Lett. **74**, 936 (1995).

[25] M. Durandurdu and D.A. Drabold, Phys. Rev. B **65**, 104208 (2002).

[26] W. Jin, R.K. Kalia, P. Vashishta, and J.P. Rino, Phys. Rev. Lett. **71**, 3146 (1993).

[27] J. Fabian and P.B. Allen, Phys. Rev. Lett. **79**, 1885 (1997).

[28] D.W. Dean, R.M. Wentzcovitch, N. Keskar, J.R. Chelikowsky, and N. Binggeli, Phys. Rev. B **61**, 3303 (2000).

[29] N. Binggeli and J.R. Chelikowsky, Phys. Rev. Lett. **69**, 2220 (1992).

[30] D.J. Lacks, Phys. Rev. Lett. **80**, 5385 (1998).

[31] V.V. Brazhkin, A.G. Lyapin, O.V. Stalgorova, E.L. Gromnitskaya, S.V. Popova, and O.B. Tsiok, J. Non-Cryst. Solids **212**, 49 (1997).

[32] S.N. Taraskin and S.R. Elliot, Phys. Rev. B **56**, 8605 (1997).

[33] B.B. Laird and S.D. Bembenek, J. Phys.: Condens. Matter **8**, 9569 (1996).